Collisions of H^+, H_2^+, H_3^+, ArH^+, H^-, H, and H_2 with Ar and of Ar^+ and ArH^+ with H_2 for Energies from 0.1 eV to 10 keV

A.V. Phelps

Joint Institute for Laboratory Astrophysics, University of Colorado, Boulder, Colorado 80309–0440

Received December 30, 1991; revised manuscript received March 23, 1992

Graphical and tabulated data and the associated bibliography are presented for cross sections for elastic, excitation, and ionization collisions of H^+, H_2^+, H_3^+, ArH^+, H^-, H, and H_2 with Ar and of Ar^+ and ArH^+ with H_2 for laboratory energies from 0.1 eV to 10 keV. Where appropriate, drift velocities and reaction or excitation coefficients are calculated from the cross sections and are recommended for use in analyses of swarm experiments and electrical discharges. In the case of H^+ in Ar, cross sections for momentum transfer, charge transfer, electronic excitation, and electron production are recommended. Drift velocity calculations predict runaway for H^+ in Ar for electric field to gas density ratios E/n greater than 4.3×10^{-18} V m^2. For H_2^+ in Ar, the cross sections include those for ArH^+ formation, charge transfer, electronic excitation, and electron production. Drift velocities and average cross sections are calculated versus E/n. In the case of ArH^+ collisions with Ar, only cross sections for ion molecule reactions are recommended. For H^- collisions with Ar only collisional detachment data is available. Momentum transfer, electronic excitation, and electron production cross section data are available for collisions of H with Ar. Collisions of H with Ar are of especial interest because of the very large cross sections for excitation of the H atoms at low energies. For H_2 in Ar cross sections for momentum transfer and excitation of the Hα and Hβ lines are recommended. For Ar^+ collisions with H_2, cross sections for charge transfer and ion molecule reactions are recommended. Cross sections for proton transfer are available for ArH^+ in H_2.

Key words: argon; charge transfer; cross section; data compilation; dissociation; electronic excitation; electron production; emission; fast neutrals; hydrogen; ionization; ions; momentum transfer; swarm coefficient.

Contents

List of Tables

List of Figures

1. Introduction

This paper presents graphical and tabulated data and the associated bibliography for cross sections for elastic, excitation, and ionization collisions of H^+, H_2^+, H_3^+, ArH^+, H^-, H, and H_2 with Ar and of Ar^+ and ArH^+ with H_2 for laboratory energies from 0.1 eV to 10 keV. Ion transport and reaction coefficients calculated from these cross sections are compared with available experimental data and are tabulated. The results presented here are a continuation of similar compilations for hydrogen ions and neutrals[1] in H_2, nitrogen ions and neutrals[2] in N_2, and argon ions and neutrals[2] in Ar.

The choices of published data for consideration were guided by their intended use in the modeling of electrical discharges in weakly ionized, low pressure H_2 and Ar mixtures. Collisions of H with Ar are of special interest because of the very large cross sections for excitation of the H atoms at low energies.[3-5] As a result Ar, and other heavy rare gases,[3] serve as indicators of atomic hydrogen in discharges. The data have been used in models of dc and transient emission measurements for low current, low pressure discharges[6] in H_2–Ar mixtures. The data are also needed in models of plasma processing discharges, such as used for the preparation of diamond-like thin films.[7] Green and McNeal,[8] Tawara and Russek,[9] and Tawara[10] have reviewed cross section data for H^+ and H collisions with Ar at energies above 1 keV. To the best of our knowledge there are no previous reviews that include recommended cross sections for hydrogen ions and neutrals in Ar or for argon ions and neutrals in H_2 at energies between thermal and about 1 keV. This compilation supersedes our previous brief review.[11]

This paper is an effort to provide data of current need and is subject to revision as new data become available. The published cross sections have been interpolated and extrapolated where necessary to provide the data needed for the models. We have not attempted to assign estimates of accuracy to the recommended data, but we have indicated areas of greater uncertainty and where extrapolations and interpolations were made. We have not considered three-body collision processes. Where a series of references are available, we have cited only those utilized and the more recent papers. A copy of our working bibliography is available on request.

The cross sections and the transport and reaction coefficients for hydrogen ions and neutrals and for ArH^+ in Ar are shown in Figs. 1 through 7 and are listed in Tables 1 through 7. The cross sections assembled from published experimental data for Ar^+ in H_2 are shown in Fig. 8 and Table 8.

Unless otherwise specified, all energies are laboratory energies ϵ rather than relative, center-of-mass, or "collision" energies. The same logarithmic energy scale is used in all of the cross-section and energy-loss tables because of the wide range of energies considered and the resultant simplicity of averages over the ion and fast neutral energy distributions. Although some entries in the tables are given to several significant figures, all entries should be considered uncertain to at least ± 5%. Blank entries in the tables indicate that the cross sections are too small to be evaluated, or are zero. In general, the curves and tables are labeled by the experimentally observed or theoretically postulated product of the collision.

2. Symbols

The symbols used in this paper are:

A	number of atoms and ions in projectile.
A'	number of atoms in target.
Dn	product of diffusion coefficient and gas density in $m^{-1}\ s^{-1}$.
E/n	electric field to gas density ratio in V m^2.
$I(\Theta)$	differential scattering cross section in $m^2\ str^{-1}$.
J	quantum number of rotational level of H_2 or H_2^+.
$L_m(X)$	momentum loss function for ion X in momentum balance model in eV m^2.
$L_s(X)$	energy loss function for ion X in energy balance model in eV m^2.
M	mass of projectile in atomic units.
M'	mass of target in atomic units.
n	gas density in molecules/m^3.
Q_{CT}	cross section for charge transfer collisions in m^2.
$Q(e)$	total cross section for electron production in m^2.
$Q(\lambda)$	total cross section for production of photons of wavelength λ in m^2.
Q_m	momentum transfer cross section in m^2.
Q_{pt}	proton transfer cross section in m^2.
$Q(k)$	cross section for process k in m^2.
Ry	Rydberg of energy = 13.6 eV.
v	quantum number of vibrational level of H_2 or H_2^+ molecule.
$W(H^+)$	drift velocity of H^+ in Ar in m/s.
$W(H_3^+)$	drift velocity of H_3^+ in Ar in m/s.
Z	effective charge of projectile in units of electron charge.
Z'	effective charge of target in units of electron charge.
$\alpha/n(k)$	spatial reaction or excitation coefficient for process k in m^{-1}.
ϵ	projectile energy in the laboratory frame in eV.
$\epsilon(X)$	drift energy of ion X in eV.
ϵ_k	energy loss in excitation of the kth level in eV.
η	dimensionless screening parameter.
μn	ion mobility normalized to unit density in $(mV\ s)^{-1}$.

3. H^+ Collisions with Ar

Many experimental and theoretical investigations of the scattering of H^+ by Ar have been published.[8-26] We are concerned only with those giving data on large angle scattering or inelastic collisions at $0.1 < \epsilon < 10^4$ eV. Here ϵ is the projectile energy in the laboratory system of

coordinates and the target kinetic energy is negligible. The momentum transfer cross sections Q_m shown in Fig. 1 and listed in Table 1 for $\epsilon_L < 1$ eV were calculated using the spiraling radius[12] and average polarizability from McDaniel and Mason.[13] Evidence for the applicability of polarization-dominated scattering for low energy H^+ in rare gases has been obtained by Orient[14] for H^+ in He and Ne. These data also suggest that the mobility of H^+ in the rare gases decreases with increasing ion energy corresponding to a slowly increasing product of momentum transfer cross section and speed. Here the density normalized mobility[13] μn is equal to the ratio of the ion drift velocity to E/n and is inversely proportional to Q_m.[1] Relative differential scattering cross section measurements[15] at energies near 10 eV are not useful in the present context. The $Q_m(H^+,Ar)$ value shown for $\epsilon_L = 1500$ eV was obtained from the elastic differential scattering cross section of Abignoli *et al.*[16] by extrapolating their data to higher scattering angles so as to merge smoothly with the differential scattering predicted using the formulas for screened Coulomb collisions[13,17] and then integrating over angle with the appropriate angular weight. This fitting procedure leads to an effective nuclear charge of $Z' = 2.3$ for Ar and to a screening parameter $\eta = 5 \times 10^{-3}$. These parameters were then used to calculate Q_m at energies ≥ 500 eV using the relation

$$Q_m(\epsilon) = 2\pi\left[\frac{ZZ'a_0R_y}{\epsilon}\frac{(m+M)}{M}\right]^2\left[\ln\left(\frac{1+\eta}{\eta}\right) - \frac{1}{(1+\eta)}\right]AA' \quad (1)$$

where m and M are the masses of the projectile and target, Z and Z' are the effective charges of the projectile and target, a_0 and Ry are the Bohr radius and the Rydberg energy, ϵ is the projectile laboratory energy, and A and A′ are the numbers of atoms in the projectile and target molecules. The small value of Z' corresponds to very little penetration of the outer shell of electrons of the Ar atom. The Q_m values for H^+–Ar shown by the short dashed curve of Fig. 1 are obtained by a smooth interpolation between the low and high energy Q_m values. Inelastic collisions dominate the large angle scattering for higher energies so that, for example, at 6 keV the total Q_m calculated by extrapolating the data of Crandall, McKnight, and Jaecks[18] to all angles using the screened approximation is 6×10^{-23} m^2.

Although the measurements[19] of cross sections for charge transfer collisions of H^+ with Ar agree reasonably well for energies above 200 eV, experiments using various techniques[19,20] disagree by about an order of magnitude near 100 eV. Very possibly the problem arises because for $\epsilon > 100$ eV the probability of large angle scattering, represented by Q_m in Fig. 1, becomes larger than that for charge transfer. At energies below 70 eV we find only the data of Maier.[20]

Cross sections are shown in Fig. 1 and are listed in Table 1 for excitation of the Lyman α (Lyα) and Balmer α (Hα) lines of H. For the excitation of Lyα we have adopted the excitation cross sections recommended by Van Zyl, Gealy, and Neuman.[21] For Hα excitation we show the results of Risley, de Heer, and Kerkdijk[22] for $\epsilon > 2$ keV. Since the only lower energy results are in a paper[23] for which the results seem to be seriously in error for other gases, e.g., H^+ and H_2^+ collisions with H_2, we have extended the higher energy data to lower energies using the energy dependence from the Lyα data. Excitation of higher levels of H has also been observed[22,24] at energies above about 1 keV. Excitation cross sections for Ar II emission have been reported[3,25] for energies above 2 keV.

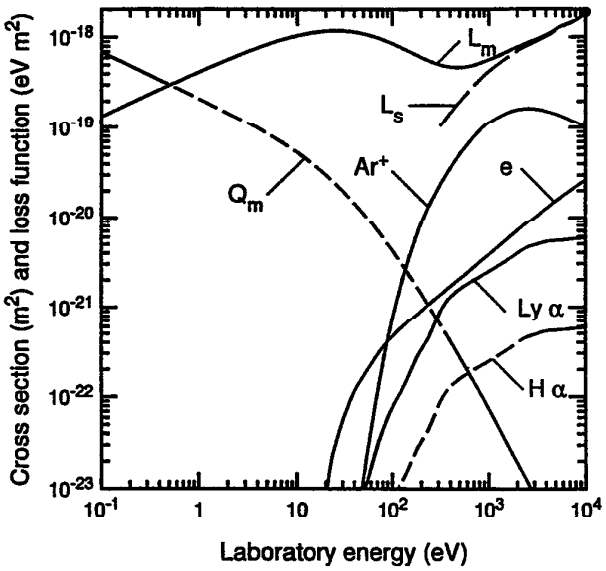

FIG 1. Cross sections and momentum loss for collisions of H^+ with Ar versus laboratory energy of H^+ for Ar at rest. The symbols and collision processes are: Q_m, momentum transfer; Ar^+, charge transfer to form Ar^+; e, electron production by ionization of Ar; Lyα, production of Lyman α radiation; and Hα, production of the Balmer α line. The curve labeled L_m is the momentum loss function and that labeled L_s is the stopping power for H^+ in Ar.

We have taken the electron production cross section $Q(e)$ to be equal to that for ionization as given by Rudd *et al.*[26]

Figure 1 and Table 1 also show the calculated momentum loss function L_m for use in a momentum balance for H^+ drifting through Ar under the action of an electric field. The momentum loss function L_m is to be distinguished from the more familiar energy loss function or stopping power[1,8–10] L_s used in models of heavy particle energy loss. It was shown in Ref. 1 that the use of L_m in a momentum balance leads to useful predictions of the drift velocities and spatial reaction coefficients as a function of E/n. Such results are shown by the solid curves of Fig. 2 and listed in Table 2. As predicted[1] for H^+ in H_2,

TABLE 1. Cross sections and loss functions for H^+ in Ar tabulated by product. The ion energies are in eV and the cross sections are in 10^{-20} m^2 and loss functions are in 10^{-20} eV m^2

Process energy loss[a] Lab. energy	Ar^+ 2.16	Lyα 10.2	Hα 12.09	Ioniz. 15.76	Q_m	Total $L_s(E)$
0.1	[b]				69	13.4
0.133					60	15.5
0.178					52	17.9
0.24					45	21
0.32					38	24
0.42					33	27
0.56					29	31
0.75					25	36
1.00					21	41
1.33					18.2	47
1.78					15.6	54
2.4					13.3	61
3.2					11.2	69
4.2					9.4	78
5.6					7.9	86
7.5					6.5	95
10.0					5.3	103
13.3					4.2	110
17.8				0.0002	3.3	115
24				0.0024	2.5	117
32				0.0063	1.88	116
42	0.0003	0.00035	0.000035	0.0126	1.36	112
56	0.0029	0.00133	0.000133	0.0205	0.96	105
75	0.016	0.0036	0.00036	0.032	0.65	96
100	0.071	0.0076	0.00076	0.046	0.43	85
133	0.23	0.013	0.00134	0.062	0.28	74
178	0.6	0.026	0.00262	0.081	0.172	64
237	1.3	0.045	0.00445	0.106	0.106	55
316	2.3	0.089	0.0089	0.137	0.064	50
422	3.8	0.14	0.0136	0.177	0.038	47
562	5.9	0.17	0.0172	0.227	0.022	47
750	8.5	0.21	0.0207	0.295	0.013	50
1000	11.3	0.25	0.0247	0.38	0.0074	57
1334	13.6	0.30	0.0295	0.49	0.0042	64
1778	15.6	0.36	0.036	0.63	0.0024	73
2370	16.5	0.45	0.0445	0.82	0.0014	84
3160	16.4	0.50	0.0495	1.03	0.00078	95
4220	15.3	0.54	0.0537	1.32	0.00044	108
5620	13.8	0.55	0.055	1.68	0.00025	130
7500	12	0.57	0.057	2.12	0.00014	148
10000	10.3	0.58	0.058	2.65	0.000079	177

[a]The energies cited are in eV and are those used in the calculation of L_m and L_s.
[b]A blank entry means the cross section is zero or too small to be estimated.

the maximum value of L_m in Fig. 1 is equal to the E/n value at which the drift velocity and ion drift energy increase without limit for $\epsilon(H^+) < 10$ keV, i.e., the E/n at which the ion runaway[1] occurs. In weakly ionized gases ion or electron runaway refers to the nonequilibrium situation in which an ion or electron gains more energy from the electric field than it loses in collisions with the gas and so continues to accelerate throughout the energy range of interest.

The stopping power L_s for H^+ in Ar is calculated as described in Ref. 1 and is shown by the curve and entries marked L_s in Fig. 1 and Table 1. The energies cited in the second row of Table 1 are the energies in eV used in the calculation of L_s for the hydrogen. Note that the energies cited for simultaneous charge transfer and excitation do not include the difference in ionization potentials for H and Ar, since this energy loss is already assigned to the total charge transfer cross section. Although the experimental stopping power value of Phillips[27] for $\epsilon = 10$ keV is in good agreement with this calculation, such a comparison is not a valid test of our cross section set because the hydrogen spends only about 20% of its time as H^+ while traveling through high densities of Ar.

TABLE 2. Drift velocities, energies, and reaction coefficients for H^+ and H_3^+ in Ar. The spatial reaction coefficients $\alpha/n(ArH^+)$ and $\alpha/n(Ar^+)$ are for H_3^+ collisions with H_2

E/n 10^{-21}Vm^2	$W(H^+)$ m/s	$\epsilon(H^+)$ eV	$W(H_3^+)$ m/s	$\epsilon(H_3^+)$ eV	$\alpha/n(ArH^+)$ m^2	$\alpha/n(Ar^+)$ m^2
150	4900	0.125	NA[a]	NA	NA[b]	NA
200	6300	0.22	NA	NA	NA[b]	NA
300	9400	0.50	3300	0.17	1.7E−19[c]	0.0
500	16800	1.5	5100	0.41	9E−20[c]	0.0
700	25000	3.3	6900	0.72	5.0E−20	0.0
1000	41000	8.6	9300	1.35	4.9E−20	1E−22
1100	50800	13	10300	1.6	4.4E−20	2E−21
1170	runaway	runaway	10800	1.8	4.2E−20	5E−21
1500			13700	3.0	3.2E−20	1.6E−20
2000			19000	5.6	2.2E−20	2.9E−20
2500			27000	11.5	1.1E−20	3.0E−20
2780			runaway	runaway	runaway	runaway

[a]NA means not available from this calculation because ϵ is below 0.1 eV.

[b]See Villinger *et al.* for rate coefficient data.[39]

[c]Here 1.7E−19 means 1.7×10^{-19}. These two entries are calculated from rate coefficients of Villinger *et al.*[39] and our drift velocities W and drift energies ϵ, while our model gives zero for these E/n. The discontinuities in the variation of $\alpha/n(ArH^+)$ values with E/n above $E/n = 5 \times 10^{-19}$ V m2 indicates that our monoenergetic-beam, momentum-balance model[1] underestimates the spatial reaction coefficients at these lower E/n. This problem is also discussed in Sec. 5.2 of Ref. 1.

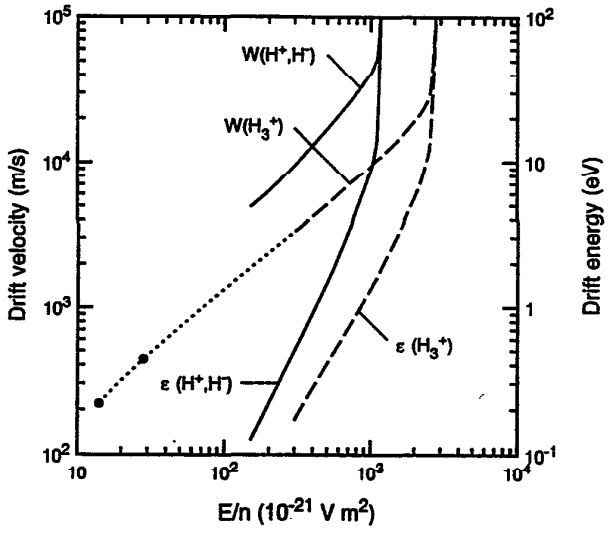

FIG 2. Drift velocities W and energies $\epsilon(X)$ for H^+, H^-, and H_3^+ ions in Ar. The solid curves are for H^+ and H^-, while the dashed curves are for H_3^+. Note that the H^+ and H^- drift velocities and energies are identical in the present set of cross sections. The dotted curve is an interpolation between the experimental points and the model for H_3^+.

4. H_2^+ Collisions with Ar

Figure 3 and Table 3 show and list reaction, excitation, and electron production cross sections for H_2^+ in Ar. The low energy behavior[28] is dominated by the proton transfer reaction leading to the formation of ArH^+ and has a cross section of about 80% of the polarization limit.[13] At energies above 6 eV we have adopted the rapid decrease in this cross section found recently by Liao *et al.*,[28] rather than the slow decrease found for D_2^+ + Ar by Smith *et al.*[29] Liao *et al.*[28] find this cross section to be approximately independent of the vibrational level of the H_2^+, although Houle *et al.*[30] found cross sections for $v = 0$ to be much smaller than for higher v levels. For energies above about 5 eV the charge transfer reaction[28,31] leading to Ar^+ formation dominates and varies slowly with the vibrational level of the incident H_2^+. At energies below about 2 eV the cross sections for this reaction are a maximum[28] for the $v = 2$ level of H_2^+. As the H_2^+ energy approaches zero the charge transfer cross section is taken to be approximately equal to the difference between that for ArH^+ formation and the polarization cross section.

The cross section for collision induced dissociation[28] in the 1–10 eV range increases rapidly as the vibrational level of the H_2^+ increases, e.g., the dissociation cross section peaks at $\epsilon \approx 6$ eV at 1.3 and 2.7×10^{-20} m^2 for $v = 1$ and 2, respectively. At energies above 2 keV we use the data of Williams and Dunbar,[32] but this leaves the range from 10 eV to 2 keV with a large uncertainty. The cross sections shown in Fig. 3 and listed in Table 3 are for the $v = 0$ level of H_2^+. One reason for the interest in vibrationally excited H_2^+ is that electron impact ionization produces a range of vibrationally excited levels.[33] At the higher energies charge transfer results in small angle collisions, i.e., $Q(Ar^+) \gg Q_m$, and so produces fast H_2.[30] We have found no information on the production of fast H in H_2^+ + Ar collisions.

The cross section for electron production shown in Fig. 3 and Table 3 is from Gordeev and Panov[34] at energies near 10 keV and from Gilbody and Hasted[35] for energies below 1 keV with a linear interpolation at intermediate energies where the experiments disagree by a factor of 2.5. The cross section for Lyα excitation is based on Ottinger and Yang[36] for $\epsilon < 900$ eV and on Van Zyl *et al.*[37] for higher energies. We have found no information on the excitation of Hα in H_2^+ + Ar collisions.

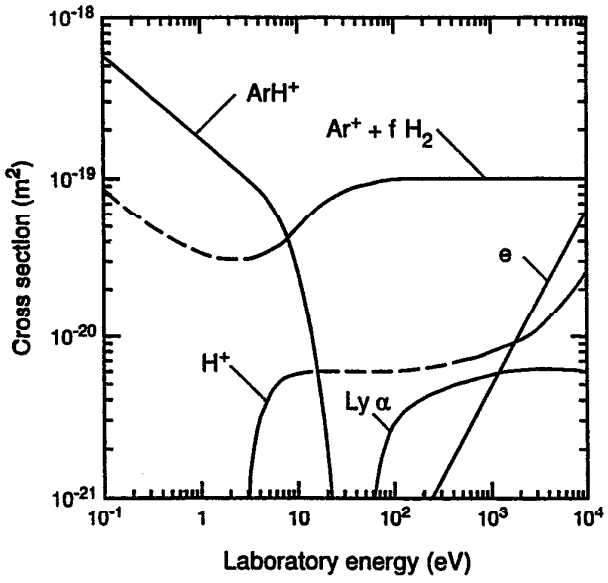

FIG 3. Cross sections for collisions of H_2^+ with Ar versus laboratory energy of H_2^+ for Ar at rest. The symbols and collision processes are: ArH^+, proton transfer to form ArH^+; Ar^+ + fast H_2, charge transfer to form Ar^+ and fast H_2; H^+, dissociation to form H^+; Lyα, production of Lyman α radiation; and e, production of electrons by ionization.

TABLE 3. Cross sections for H_2^+ collisions with Ar tabulated by product. The ion energies are in eV and the cross sections are in 10^{-20} m^2

Process Lab. energy	ArH^+	Ar^+	H^+	Lyα	e+Ar^+
0.1	58	8.6			
0.1334	50	7.4			
0.1778	43	6.4			
0.237	37	5.65			
0.316	31.7	4.95			
0.422	27.5	4.45			
0.562	23.6	4			
0.750	20.3	3.67			
1	17.5	3.38			
1.334	15.1	3.19			
1.778	13	3.1			
2.37	11.2	3.09			
3.16	9.6	3.11	0.14		
4.22	8.15	3.3	0.33		
5.62	6.4	3.6	0.47		
7.50	4.55	4.05	0.55		
10	2.57	4.9	0.58		
13.34	1.15	5.9	0.595		
17.78	0.36	6.9	0.6		
23.7	0.066	7.7	0.6		
31.6	0.001	8.4	0.6		
42.2		8.95	0.6	0.01	
56.2		9.3	0.6	0.07	
75.0		9.7	0.6	0.185	0.027
100		9.9	0.605	0.287	0.037
133.4		10	0.61	0.35	0.051
177.8		10	0.625	0.395	0.066
237		10	0.64	0.435	0.099
316		10	0.66	0.465	0.138
422		10	0.69	0.5	0.19
562		10	0.72	0.523	0.264
750		10	0.75	0.55	0.365
1000		10	0.805	0.575	0.5
1334		10	0.86	0.6	0.69
1778		10	0.92	0.61	0.95
2370		10	1	0.62	1.29
3160		10	1.13	0.625	1.78
4220		10	1.35	0.625	2.45
5620		10	1.64	0.62	3.36
7500		10	2.03	0.615	4.65
10000		10	2.6	0.6	6.3

The concept of ion drift velocity has no significance for H_2^+ in Ar because of the rapid destruction of H_2^+ by reactions to form ArH^+ or H_2^+. We therefore have no ion mobility data that can be used to obtain the momentum transfer cross section at low energies. At energies above about 500 eV, Eq. (1) leads to a momentum transfer cross section only slightly larger than that for H^+ + Ar collisions as shown in Fig. 1. It is important to keep in mind that for drift tube experiments[6] at $E/n > 10^{-18}$ V m^2 the energy gained by the H_2^+ between collisions with the Ar is large enough, i.e., $(E/n)/\Sigma Q(\epsilon) > 10$ eV, so that the product of a collision of H_2^+ with Ar is Ar^+ rather than ArH^+. Here $\Sigma Q(\epsilon)$ is the sum of all H_2^+–Ar cross sections.

5. H_3^+ Collisions with Ar

Figure 4 and Table 4 show the cross sections for H_3^+ collisions with Ar. The estimated momentum transfer cross section Q_m at low ϵ is based on the mobility measurements of McAfee, Sipler, and Edelson.[38] Their mobility value for H_3^+ in Ar at low E/n corresponds to a significantly higher Q_m than calculated from the polarizability of Ar.[13] We have shown two limiting forms for $Q_m(\epsilon)$ by the long dashed lines in Fig. 1, i.e., constant Q_m and constant $vQ_m(\epsilon)$. Here v is the ion speed. At $\epsilon > 500$ eV we have used the scaling of Eq. (1) to estimate the contribution of elastic collisions to Q_m. We have no information regarding the inelastic contribution corresponding to that found[18] to be dominant at high energies for H^+ in Ar. At intermediate energies we have interpolated between the low and high energy cross sections.

The cross sections for the formation of ArH^+ in H_3^+ + Ar collisions shown in Fig. 4 and Table 4 have been estimated from reaction rate coefficients calculated from equilibrium coefficients and from rate coefficients for the reverse reaction of ArH^+ with H_2 measured by Villinger *et al.*[39] The energy dependence at $\epsilon > 10$ eV is based on the measurements of Prokof'ev *et al.*[40] for D_3^+ collisions with Xe and on the ArH^+ formation data for H_2^+ + Ar of Sec. 4.

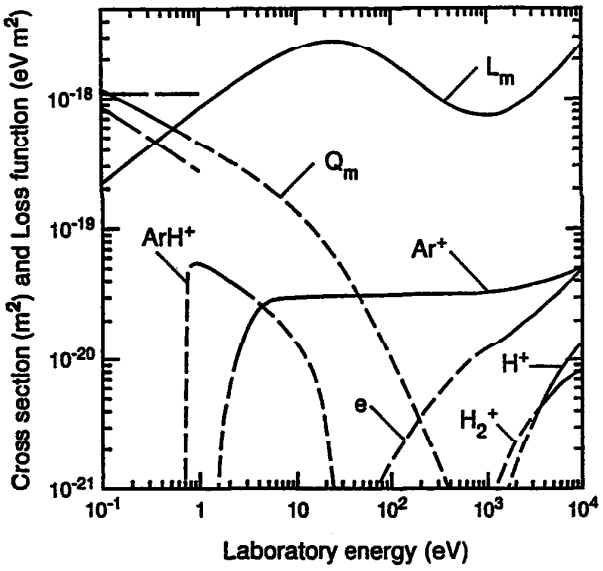

FIG 4. Cross sections and momentum loss for collisions of H_3^+ with Ar versus laboratory energy of H_3^+ for Ar at rest. The symbols and collision processes are: Q_m, momentum transfer; ArH^+, proton transfer to form ArH^+; Ar^+, charge transfer to form Ar^+; H^+, dissociation to form H^+; H_2^+, dissociation to form H_2^+; and e, production of electrons by ionization. The curve labeled L_m is the momentum loss function.

The charge transfer cross section for formation of Ar^+ shown in Fig. 4 and Table 4 is from Prokof'ev *et al.*[40] for $\epsilon < 40$ eV and from Gordeev and Panov[34] for $\epsilon > 1$ keV. The latter authors report cross sections for electron capture in $H_3^+ + Ar$ collisions for $\epsilon > 1$ keV, but the product neutral is unknown and so is not shown in Fig. 4. The cross sections for dissociation of H_3^+ into H^+ and H_2^+ for $\epsilon > 3$ keV are from Williams and Dunbar.[32] The excitation of Lyα or Hα does not appear to have been observed for $\epsilon < 10$ keV. The cross section shown for the production of electrons in collisions of H_3^+ with Ar is also from Prokof'ev *et al.*[40]

The $Q_m(\epsilon)$ estimate shown in Fig. 4 and Table 4 is used to calculate the loss function $L_m(\epsilon)$ and the H_3^+ drift velocities W and ion drift energies $\epsilon(H_3^+)$ shown by the dashed curves of Fig. 2 and listed in Table 2. At low E/n we show that the calculated drift velocities extrapolate via the dotted curve to the low E/n limit of the data of McAfee, Sipler, and Edelson.[38] At $E/n \approx 2.8 \times 10^{-18}$ V m^2 runaway occurs when L_m for H_3^+ in Ar passes through a maximum. We have no experimental data at such high E/n and, in the absence of more accurate transport calculations, can only suggest the onset of runaway. Note that once the H_3^+ energies reach about 40 eV ($E/n > 2.8\ 10^{-18}$ V m^2), ion destruction by charge transfer exceeds large angle elastic scattering and the concept of drift velocity is no longer useful.

We recommend the rate coefficient data of Villinger *et al.*.[39] for the $H_3^+ + Ar \rightarrow ArH^+ + H_2$ reaction as obtained from measurements of the rate coefficients for the reverse reaction and of equilibrium constants versus E/n. However, it should be noted that there are serious, unresolved discrepancies between the equilibrium constant data measured by Villinger *et al.*[39] and the equilibrium constants we derive from the dependence on fractional H_2 concentration of the mean ion drift velocity found by McAfee *et al.*[38]

6. ArH^+ Collisions with Ar

Ion mobility measurements for ArH^+ in Ar have been reported by McAfee *et al.*[38] and by Rakshit and Warnek.[41] Since Villinger *et al.*[39] have suggested that the interpretation of the latter data is in error because of neglect of the back reaction of H_3^+ with H_2, we base our $Q_m(\epsilon)$ recommendation at low energies on McAfee *et al.*[38] Further support for this concern is provided by noting that the much higher apparent mobility of H_3^+ in Ar found by Rakshit and Warneck[41] compared to that of McAfee *et al.*[38] is just about what one would expect for the fractional H_2 concentration and E/n used by Rakshit and Warneck[41] and for the equilibrium constants for the forward and reverse reactions of H_3^+–ArH^+ in H_2–Ar mixtures derived from McAfee *et al.*[38] As indicated by Lindinger and Albritton[42] the mobility of ArH^+ in Ar at low E/n is 70% of the value calculated using the polarizability of Ar. Thus, if we assume νQ_m is constant then $Q_m(\epsilon) = 4.4 \times 10^{-19}\,\epsilon^{-1/2}$ m^2 for ArH^+ collisions with Ar, where ϵ is in eV.

We have not found any other data for the collisions of ArH^+ with Ar. Reactions of potential importance for accurate modeling of low pressure, gas discharges in Ar–H_2 mixtures are the dissociation of ArH^+ in collisions with Ar and the charge transfer of ArH^+ with Ar to form Ar^+. Claims of measurement of the rate of relaxation of internal energy[41] of ArH^+ in Ar are suspect as discussed above for the mobility.

7. H^- Collisions with Ar

The momentum transfer cross section shown for H^- collisions with Ar in Fig. 5 and listed in Table 5 is the same as that for H^+ in Ar discussed in Sec. 1. Since there appears to be no relevant experimental data, this choice is based on the assumed dominance of the polarization interaction at low energies and of a Coulomb interaction at high energies. It should be pointed out, however, that calculations[43] for H^- in He show that at low energies there is a decrease in the effective product of speed and Q_m for increasing energy caused by a repulsive interaction, such as calculated[43] for H^- interaction with both He and Ar. Thus, the energy dependence of Q_m for H^- in Ar may be rather different than that for the attractive interaction for H^+–He.

For ϵ above about 10 eV the dominant collision process for H^- in Ar is collisional detachment of the electron as shown in Fig. 5 and Table 5. Experimental data have been tabulated by Tawara[10] and tabulated and reviewed

TABLE 4. Cross sections and loss functions for H_3^+ in Ar tabulated by product. The energies are in eV and the cross sections are in 10^{-20} m^2 and loss functions are in 10^{-20} eV m^2

Process	$ArH^+ + H_2$	$Ar^+ + H$	$H^+ + H_2$	$H_2^+ + H$	e	Q_m	L_m
Energy loss[a]	0.6	4.6	6.4	4.4	13.6		
Lab. energy							
0.100						118	22
0.133						105	26
0.178						93	31
0.237						83	37
0.316						74	43
0.422						65	51
0.562						58	61
0.750	5					51	72
1.000	5.4					45	84
1.33	4.9	0.01				40	99
1.78	4.25	0.39				35	115
2.37	3.64	1.03				30	134
3.16	3.12	1.88				26	155
4.22	2.6	2.6				23	177
5.62	2.16	2.9				19.1	200
7.50	1.72	3.0				16.0	223
10.0	1.3	3.0				13.1	244
13.3	0.9	3.0			0.008	10.5	261
17.8	0.475	3.1			0.013	8.3	273
23.7	0.11	3.1			0.0225	6.3	278
31.6	0.01	3.1			0.034	4.7	274
42.2		3.1			0.051	3.3	262
56.2		3.1			0.075	2.3	242
75.0		3.1			0.112	1.54	218
100		3.1			0.163	1.00	190
133		3.2			0.227	0.64	163
178		3.2			0.318	0.39	138
237		3.2			0.435	0.24	117
316		3.2			0.563	0.142	100
422		3.2		0.005	0.715	0.084	87
562		3.2		0.015	0.89	0.049	80
750		3.2	0.005	0.035	1.07	0.028	76
1000		3.3	0.02	0.074	1.23	0.0162	75
1334		3.4	0.057	0.12	1.39	0.0092	76
1778		3.5	0.12	0.198	1.62	0.0053	83
2370		3.6	0.21	0.287	1.93	0.0030	95
3160		3.8	0.35	0.385	2.26	0.00169	111
4220		4.0	0.55	0.49	2.73	0.00095	135
5620		4.3	0.78	0.62	3.26	0.00054	165
7500		4.7	1.05	0.735	4	0.00030	208
10000		5.1	1.35	0.83	4.9	0.00017	263

[a] The energies cited are in eV and are those used in the calculation of L_m and L_s.

by Risley.[44] We have adopted the cross section data of Champion, Doverspike, and Lam[45] for $\epsilon < 100$ eV and the results of Risley and Geballe[46] for $\epsilon > 200$ eV.

The production of electrons by double electron stripping and ionization to form $2e + H^+$ in collisions of H^- with Ar has been investigated by Williams[47] and the cross sections are shown in Fig. 5 and Table 5. The excitation[48] of $H(2s + 2p)$ and of $H\alpha$ in collisions of H^- with Ar are shown in Fig. 5. Since this excitation process is only reported for energies above 1 keV, it would appear that there is no low energy peak in the cross section for excitation of H atoms. See Sec. 8. We have therefore extended the cross sections for excitation to lower energies using the energy dependence for excitation of $Ly\alpha$ in $H^+ + Ar$ collisions. The excitation of very high lying[49] levels of H at $\epsilon > 3$ keV and the energy losses corresponding to excitation[45] of Ar in $D^- + Ar$ collisions at $\epsilon = 57$ eV have been reported.

We have found no transport data for H^- in Ar. Subject to the uncertainties in the Q_m values discussed above, the drift velocities of low energy H^- in Ar calculated using L_m will be similar to that for H^+ in Ar shown in Fig. 2. In the calculation of L_m we have used the energy losses given in the second row of Table 5. Again the concept of an equilibrium drift velocity fails for $\epsilon > 10$ eV ($E/n > 5 \times 10^{-19}$ V m^2) because of detachment and because of runaway. The large cross section for detachment relative to that for large angle scattering Q_m means that for $\epsilon > 100$ eV, detachment will result in the production of a fast H atom moving in the electric field direction.

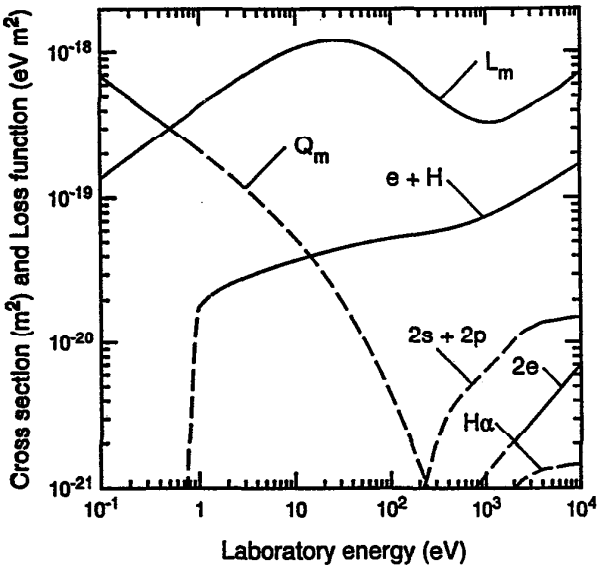

FIG 5. Cross sections and momentum loss for collisions of H^- with Ar versus laboratory energy of H^- for Ar at rest. The symbols and collision processes are: Q_m, momentum transfer; e + H, electron detachment transfer to form H; $2e$, production of electrons by detachment and ionization; $2s + 2p$, sum of production of H atoms in the $2s$ and $2p$ states; and Hα, production of the Balmer α line. The curve labeled L_m is the momentum loss function for H^- in Ar.

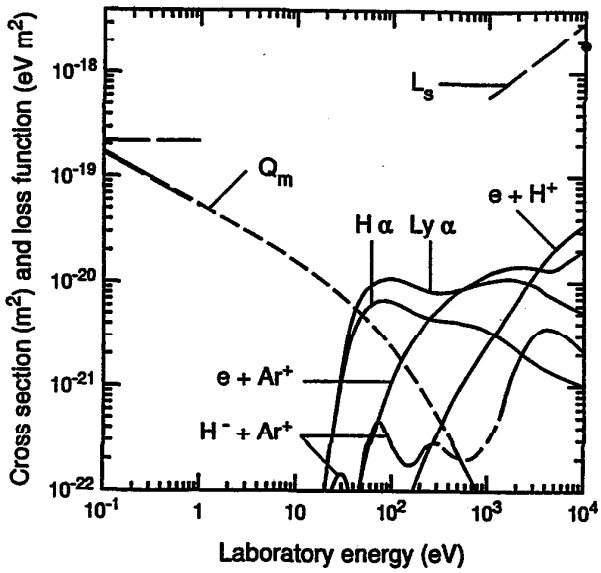

FIG 6. Cross sections and stopping power for collisions of H atoms with Ar versus laboratory energy of H for Ar at rest. The symbols and collision processes are: Q_m, momentum transfer; Lyα, production of Lyman α radiation; Hα, production of the Balmer α line; e, production of electrons by ionization to form Ar^+; e, production of electrons by ionization to form H^+. The curve labeled L_s is the stopping power for H in Ar.

8. H Collisions with Ar

The momentum transfer cross section Q_m for low energy H atoms in Ar is determined from the measured diffusion coefficient[50] at room temperature of $Dn = 3.4 \times 10^{21}\ m^{-1}s^{-1}$. We have not found any temperature dependent experimental data and so are not able to establish the energy dependence of Q_m at low energies. In principle, theoretical differential scattering cross sections[51] could be integrated to obtain energy dependent Q_m values at $\epsilon < 0.1$ eV. The long dashed lines in Fig. 6 show possible extrapolations of $Q_m(\epsilon)$ consistent with the thermal results to energies of interest here. Unfortunately, the elastic differential scattering cross sections of Gao *et al.*[52] do not extend to large enough angles to allow one to calculate Q_m. We have shown by the solid line of Fig. 6 and have listed in Table 6 values obtained using Eq. (1) for Q_m at energies above 500 eV with the parameters used for H^+ in Ar in Sec. 3. Alternatively, we can readjust the $I(\Theta)$ calculation of Van Zyl *et al.*[53] at 0.5 degree to fit an interpolation between values of $I(\Theta)$ for 500 and 1000 eV from Gao *et al.* for 0.5 degree, extrapolate the $I(\Theta)$ of Van Zyl *et al.*[53] to larger angles using screened Coulomb theory,[12] and integrate the appropriately weighted $I(\Theta)$ to find Q_m. This procedure gives $Q_m = 1 \times 10^{-22}\ m^2$ at 1000 eV, or about 50% larger than that obtained using Eq. (1) and shown in Fig. 6 and Table 6. The dashed portion of the $Q_m(\epsilon)$ curve is a smooth interpolation between the low and high energy results. The recommended data are given in Table 6.

The Lyα and Hα excitation cross sections shown in Fig. 6 and Table 6 are very large at low H atom energies. The high probability of such collisions in discharges is the principal reason for our interest in the H_2–Ar system. The cross sections for Lyα and Hα excitation shown are from the experiments of Van Zyl *et al.*[4] and Van Zyl and Gealy.[5]

The charged particle production cross sections, i.e., those for formation of $H^- + Ar^+$, $e + H^+ + Ar$, and $e + Ar^+ + H$, shown in Fig. 6 and Table 6 are from the measurements and analyses of Van Zyl *et al.*[53] The cross sections for ion pair formation, i.e., $H + Ar \rightarrow H^- + Ar^+$, are extended to $\epsilon = 22$ eV using the relative cross sections of Aberle, Grosser, and Krüger.[54] At intermediate energies we have interpolated between the curves shown by Van Zyl *et al.*

The long dashed curve of Fig. 6 shows the stopping power for H atoms traversing Ar calculated from the cross section set of Fig. 6 and Table 6. This energy loss function or stopping power L_s is calculated using the energy losses given in the second row of Table 6. Most of these energies are approximate minimum values in center-of-mass for reactions involving the potential energy curves of the ArH molecule. The energies for Lyα and

TABLE 5. Cross sections for H^- collisions with Ar tabulated by product. The ion energies are in eV and the cross sections are in 10^{-20} m^2 and loss functions are in 10^{-20} eV m^2

Process Energy loss[a] Lab. energy	e+H+Ar 0.754	2s+2p 10.2	Hα 12.09	2e+H⁺+Ar 16.6	Q_m	Total $L_m(E)$
0.1					68.9	13.44
0.1334					59.6	15.50
0.1778					51.5	17.88
0.237					44.5	20.6
0.316					38.5	23.7
0.422					33.2	27.3
0.562					28.7	31.4
0.750					24.7	36.1
1.000	1.82				21.2	42.8
1.334	2.17				18.20	49.0
1.778	2.44				15.56	55.8
2.37	2.67				13.25	63.3
3.16	2.89				11.22	71.4
4.22	3.10				9.44	80.0
5.62	3.31				7.87	88.9
7.50	3.52				6.49	97.7
10.00	3.73				5.28	105.9
13.34	3.94				4.22	112.8
17.78	4.15			0.0008	3.31	117.9
23.7	4.36			0.0031	2.53	120.3
31.6	4.56			0.0054	1.884	119.8
42.2	4.76	0.0009	0.00009	0.0080	1.362	115.8
56.2	4.94	0.0035	0.00033	0.0111	0.955	108.8
75.0	5.11	0.0094	0.0009	0.0148	0.650	99.4
100.0	5.28	0.0199	0.0019	0.0194	0.429	88.3
133.4	5.43	0.0351	0.0034	0.025	0.275	76.8
177.8	5.58	0.0686	0.0066	0.032	0.1724	65.7
237	5.75	0.1166	0.0111	0.040	0.1056	55.8
316	5.95	0.233	0.022	0.051	0.0636	48.2
422	6.19	0.356	0.034	0.063	0.0377	42.3
562	6.50	0.451	0.043	0.079	0.0221	37.6
750	6.91	0.542	0.052	0.099	0.0128	34.5
1000	7.42	0.647	0.062	0.123	0.0074	33.0
1334	8.05	0.773	0.074	0.154	0.0042	33.2
1778	8.82	0.943	0.090	0.191	0.0024	35.2
2370	9.73	1.166	0.111	0.237	0.00137	39.2
3160	10.79	1.297	0.124	0.295	0.00078	43.3
4220	12.02	1.407	0.134	0.366	0.00044	48.6
5620	13.43	1.441	0.138	0.455	0.00025	54.6
7500	15.03	1.493	0.143	0.565	0.00014	62.7
10000	16.84	1.520	0.145	0.701	0.000079	72.7

[a] The energies cited are in eV and are those used in the calculation of L_m and L_s.

Hα are obtained by extrapolating the excitation cross sections[4,5] to threshold. As pointed out in Sec. 3, a hydrogen nucleus with energies below 20 keV spends most of its time as H rather than H^+ so that the measured stopping power[27] for H^+ in Ar, shown by the point in Fig. 6 for ϵ = 10 keV, should be compared with that calculated for H atoms in Ar. The discrepancy is about 60% and its source is unknown.

9. H_2 Collisions with Ar

Our recommended momentum transfer cross section for H_2 by Ar (or Ar by H_2) at low energies is obtained from the rather extensive measurements of the temperature dependent diffusion coefficients.[55] For temperatures from 240 to 1100 K, the density normalized diffusion coefficient is given to within 5% by $Dn = 5.3 \times 10^{21}\ (T/1000)^{0.8}$ $m^{-1}s^{-1}$, where the temperature is in degrees Kelvin. When substituted into transport integrals,[55] this yields $Q_m(\epsilon) = 1.17 \times 10^{-19}\ (\epsilon)^{-0.3}$ m^2. At higher energies we again have little choice but to use Eq. (1) with the parameters derived for H^+ collisions with Ar and appropriately modified masses. A smooth interpolation between these limits gives the empirical relation that $Q_m(\epsilon) = 1.17 \times 10^{-19}\ (\epsilon)^{-0.3}\ (1 + \epsilon/47.4)^{-1.7}$.

Rate coefficients for vibrational relaxation of H_2 by Ar have been measured[56,57] for temperatures from 300 to 2700 K and the results can be written in the form $k = 4 \times 10^{-10} \times \exp(-120/T^{-1/3})$ m^3/s. Theory[58] has been used to obtain thermally averaged cross sections for this pro-

TABLE 6. Cross sections for H collisions with Ar tabulated by product. The atom energies are in eV and the cross sections are in 10^{-20} m^2 and loss functions are in 10^{-20} eV m^2

Process	LyAlph	Bal Alp	$H^- + Ar^+$	$e + H^+$	$e + Ar^+$	Q_m	L_s
Energy loss[a]	15	16	15	13.6	15.76		
Lab. Energy							
0.1000						17.3	
0.1334						15.0	
0.1778						12.9	
0.237						11.2	
0.316						9.7	
0.422						8.4	
0.562						7.2	
0.750						6.3	
1.000						5.4	
1.334						4.7	
1.778						4.0	
2.37						3.5	
3.16						3.0	
4.22						2.5	
5.62						2.2	
7.50						1.83	
10.00						1.55	
13.34	0.0002	0.0002				1.29	
17.78	0.004	0.004	0.0001			1.07	
23.7	0.034	0.034	0.01			0.87	
31.6	0.2	0.16	0.014	0.0013		0.70	2.8
42.2	0.59	0.39	0.008	0.0073		0.55	6.2
56.2	0.89	0.58	0.03	0.024		0.42	10.1
75.0	1.04	0.67	0.045	0.056	0.0011	0.32	12.6
100.0	1.08	0.65	0.027	0.11	0.0026	0.23	13.1
133.4	1.01	0.58	0.019	0.2	0.0056	0.160	13.8
177.8	0.91	0.5	0.019	0.3	0.012	0.110	15.6
237	0.82	0.46	0.026	0.43	0.022	0.074	19.6
316	0.8	0.43	0.028	0.57	0.04	0.048	25
422	0.82	0.42	0.022	0.73	0.07	0.030	31
562	0.88	0.41	0.02	0.89	0.11	0.018	39
750	0.96	0.38	0.0215	1.03	0.17	0.011	48
1000	1.02	0.34	0.03	1.2	0.25	0.0066	59
1334	1.07	0.29	0.052	1.32	0.37	0.0039	72
1778	1.08	0.24	0.125	1.4	0.56	0.0023	88
2370	1.02	0.20	0.22	1.41	0.85	0.0013	108
3162	0.93	0.16	0.32	1.37	1.23	0.00074	132
4220	0.77	0.14	0.36	1.3	1.72	0.00043	159
5620	0.67	0.12	0.33	1.4	2.27	0.00024	197
7500	0.58	0.11	0.27	1.7	2.88	0.00014	250
10000	0.52	0.1	0.21	2	3.5	0.00008	308

[a]The energies cited are in eV and are those used in the calculation of L_m and L_s.

cess. Observations of energy loss caused by vibrational excitation have been reported[59] for center-of-mass energies from 37 to 150 eV, but cross sections are not given.

Cross sections for excitation of the Hα and Hβ lines of the Balmer series of H in collisions of fast H_2 with Ar, or its equivalent fast Ar with H_2, have been reported by Gusev *et al.*[60] and are shown in Fig. 7 and Table 7. Although not as large as for H + Ar, these cross sections rise rapidly at low laboratory energies and may be of considerable importance in low pressure gas discharges. Note that even though $Q_m(\epsilon)$ is an order of magnitude larger than the Hα excitation cross sections at, for example, 100 eV, the large mass ratio means a small ($\approx$ 10%) energy loss per elastic collision and a moderately high probability of excitation before energy relaxation.

We have not found cross section data for electron or ion production in collisions of H_2 with Ar for energies below 10 keV.

10. Ar^+ Collisions with H_2

Figure 8 and Table 8 show and list reaction, excitation, and electron production cross sections for Ar^+ collisions with H_2. The low energy behavior is dominated by the exothermic proton transfer reaction leading to the formation of ArH^+. For $\epsilon < 4$ eV we have based our recommended cross section Q_{pt} on a power law fit to the drift tube-flowing afterglow reaction coefficient k_{pt} data[61] for temperatures T from 20 to 5000 K that yields $k_{pt} = 1.45 \times 10^{-15} (kT)^{0.14}$ m^3/s to within 10% and $Q_{pt}(\epsilon) = 4.2 \times$

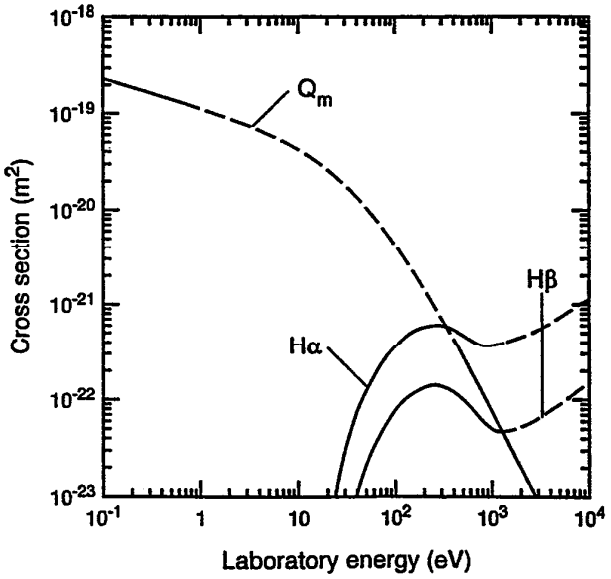

FIG 7. Cross sections and momentum loss for collisions of H_2 molecules with Ar versus laboratory energy of H_2 for Ar at rest. The symbols and collision processes are: Q_m, momentum transfer; Hα, production of the Balmer α line; and Hβ, production of the Balmer β line.

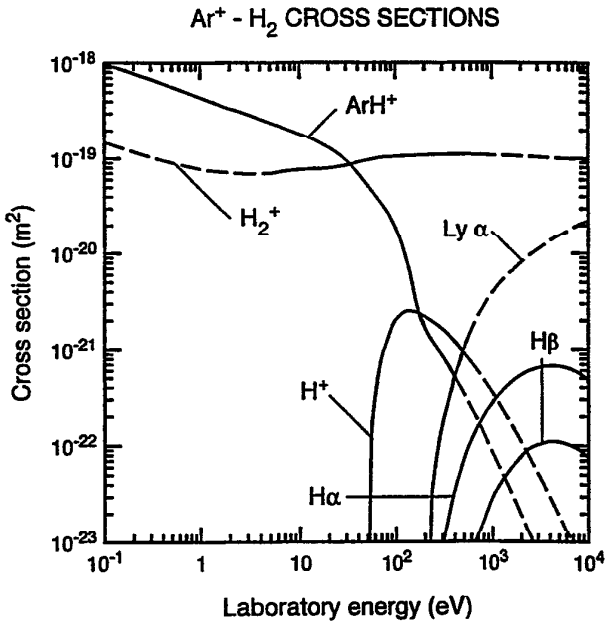

FIG 8. Cross sections and momentum loss for collisions of Ar^+ with H_2 versus laboratory energy of Ar^+ for H_2 at rest. The symbols and collision processes are: ArH^+, H atom transfer to form ArH^+; H_2^+, charge transfer to form H_2^+; H^+, dissociative charge transfer to form H^+; Lyα, production of Lyman α radiation; Hα, production of the Balmer α line; and Hβ, production of the Balmer β line.

TABLE 7. Cross sections for H_2 collisions with Ar tabulated by product. The molecule energies are in eV and the cross sections are in 10^{-20} m^2

Process Lab. energy	Hα	Hβ	Q_m
0.1			23.2
0.1334			21.3
0.1778			19.5
0.237			17.8
0.316			16.3
0.422			14.9
0.562			13.6
0.750			12.4
1.000			11.3
1.334			10.2
1.778			9.2
2.37			8.3
3.16			7.4
4.22			6.6
5.62			5.7
7.50			5.0
10.00			4.2
13.34			3.5
17.7	0.00005		2.9
23.7	0.001	0.000095	2.3
31.6	0.0036	0.00045	1.74
42.2	0.0087	0.0013	1.29
56.2	0.0155	0.00285	0.92
75.0	0.025	0.005	0.64
100.0	0.036	0.0078	0.43
133.4	0.047	0.0105	0.28
177.8	0.055	0.0125	0.174
237	0.059	0.014	0.108
316	0.059	0.0135	0.065
422	0.052	0.0115	0.039
562	0.044	0.009	0.023
750	0.037	0.0065	0.0132
1000	0.036	0.005	0.0076
1334	0.039	0.0047	0.0044
1778	0.043	0.005	0.0025
2370	0.048	0.0056	0.00142
3160	0.055	0.0066	0.00080
4220	0.065	0.008	0.00046
5620	0.078	0.0097	0.00026
7500	0.095	0.0122	0.000145
10000	0.114	0.0153	0.000082

10^{-19} $\epsilon^{-0.36}$ m^2. Here k is the Boltzmann constant and kT is in eV. At energies above 6 eV we have adopted the rapidly decreasing cross section found by Ervin and Armentrout.[62] Note that because of the large mass of the Ar ion relative to that of the target H_2, the region of polarization and proton transfer dominance extends from thermal energies up to laboratory energies ϵ of about 40 eV, i.e., center-of-mass energies of ≈ 2 eV.

The cross section for the formation of H_2^+ is usually based on a measurement of the cross section for slow ion formation.[63] The assignment to H_2^+ formation rather than ArH^+ formation is based on the lack of persistence of velocity expected of the heavy ArH^+, i.e., the ease with which the ions are collected. Since there is a very large spread in the measured cross sections, we have shown in

TABLE 8. Cross sections for Ar^+ collisions with H_2 tabulated by product. The ion energies are in eV and the cross sections are in 10^{-20} m^2

Process Lab. energy	$ArH^+ + H$	$H_2^+ + Ar$	$v=0-1$	Lyα	H_2(UV)	$H^+ + H$	Hα	Hβ
0.1	98	14.8						
0.1334	89	13.4						
0.1778	81	12.2						
0.237	73.5	11.1						
0.316	67	10.2						
0.422	60.5	9.45						
0.562	54.5	8.8						
0.750	49	8.25						
1.000	44	7.75						
1.334	39.5	7.4						
1.778	35	7.2						
2.37	32	7						
3.16	28.7	6.9						
4.22	25.7	6.95						
5.62	23	7.05						
7.50	20.3	7.4						
10.0	18.2	7.6						
13.34	16	7.75						
17.78	13.8	7.8						
23.7	11.6	8.1						
31.6	9.1	8.5						
42.2	6.6	9.2						
56.2	4.6	9.75						
75.0	3.15	10.25				0.1		
100	1.86	10.4				0.203		
133.4	0.76	10.6				0.25		
177.8	0.22	10.7				0.235		
237	0.123	10.9		0.0037	0.00005	0.195	0.00013	
316	0.079	10.95		0.021	0.00031	0.155	0.00122	0.0003
422	0.047	10.95		0.061	0.00042	0.113	0.0042	0.00047
562	0.0275	10.95		0.137	0.00059	0.08	0.0099	0.00074
750	0.0155	10.9		0.25	0.00102	0.054	0.0178	0.0014
1000	0.0085	10.75	4.7	0.39	0.00215	0.035	0.0278	0.0029
1334	0.0047	10.7	4.1	0.55		0.022	0.0387	0.0047
1778	0.0025	10.6	3.6	0.72		0.0133	0.05	0.0068
2370	0.0013	10.4	3	0.93		0.008	0.059	0.0091
3160	0.00067	10.25	2.4	1.14		0.0047	0.065	0.0103
4220	0.00035	10.1		1.4		0.0027	0.0675	0.011
5620	0.00019	9.95		1.65		0.0015	0.0657	0.0106
7500	0.0001	9.8		1.95		0.00084	0.059	0.0095
10000		9.6		2.27		0.00045	0.048	0.0075

Fig. 8 and Table 8 values calculated assuming statistical equilibrium among the $P_{1/2}$ and $P_{3/2}$ states of Ar^+ and using cross sections from the state-selected measurements by Liao *et al.*[64] These authors measured the dependence of the cross section for H_2^+ formation on the spin state of the Ar^+ and have determined the vibrational distribution of the product H_2^+ ions at energies from 50 to 400 eV. They find that there is a strong preference for excitation of $v' = 2$ by $P_{1/2}$ ions at $\epsilon < 150$ eV and for $v' = 0$ for $P_{3/2}$ ions at $\epsilon < 5$ eV, but that as the energy increases the vibrational state distribution spreads with a peak for $v' = 1$ to 3. Similar broad, but displaced, vibrational distributions have been predicted theoretically by Hedrick *et al.*[65] for $Ar^+ + H_2$ collisions at energies of 1 to 3 keV and have been found[33] for electron impact ionization of H_2.

The cross sections for charge transfer and dissociation leading to H^+ are based on Liao *et al*[64] for $\epsilon < 200$ eV and on Gustafsson and Lindholm[66] for energies up to 900 eV. This cross section increases rapidly at energies above its threshold at about 50 eV and peaks near 150 eV. We do not find data on electron production in collisions of Ar^+ with H_2 in our energy range.

The cross section shown in Fig. 8 and Table 8 for Lyα excitation is based on Ottinger and Yang[67] for $\epsilon < 700$ eV and is extrapolated smoothly to higher energies. The cross section for the production of UV emission from the H_2 $b^3\Sigma$ state from Brandt and Ottinger[68] is too small to show, but is listed in Table 8. Both of these cross sections rise rapidly near their thresholds. Cross sections for the excitation of the Hα and Hβ lines in $Ar^+ + H_2$ collisions have been reported by Gusev *et al.*[60] and are shown in Fig. 8 and Table 8.

The concept of ion drift velocity has no significance for Ar^+ in H_2 because of the rapid destruction of Ar^+ by reactions to form ArH^+ and H_2^+. We therefore could only estimate the cross section for large angle scattering from

the formulas for polarization scattering. It is important to keep in mind that for drift tube experiments[6] at $E/n > 4 \times 10^{-18}$ V m^2 the energy gained by the Ar^+ between collisions with the H_2 is large enough, i.e., $(E/n)/\Sigma Q(\epsilon) > 40$ eV, so that the product of a collision of Ar^+ with H_2 is H_2^+ rather than the ArH^+ formed in drift tubes at more lower E/n.

11. ArH^+ Collisions with H_2

The only experimental cross section or rate coefficient data we have found for collisions of ArH^+ with H_2 are for the reaction to form $H_3^+ + Ar$. Villinger *et al.*[39] obtained rate coefficients for this reaction for mean center-of-mass energies from 0.09 to 0.3 eV for ArH^+ ions drifting through Ar. As pointed out in Sec. 5, acceptance of these data requires that we discard the apparently conflicting equilibrium constants we derive from the pressure dependent mobility data of McAfee *et al.*[38] Neglect of the back reaction, i.e., $H_3^+ + Ar \rightarrow ArH^+ + H_2$, has caused serious errors in the interpretation of data.[39,41] Studies of the dynamics of $ArH^+ + H_2 \rightarrow H_3^+ + Ar$ collisions have been reported by Blakely, Vestal, and Futrell[69] for $2.5 < \epsilon < 100$ eV.

Of potential importance for analyses of discharges in H_2–Ar mixtures at low pressures and high E/n are the reactions of ArH^+ with H_2 to form H_2^+ and H^+ at energies over 100 eV. No information on these reactions is available.

12. Discussion

The wide range of processes and of energies for which cross sections are compiled in this paper illustrate the complexity of "complete" atomic models of laboratory and atmospheric plasmas. Assembly of the cross section data is only the beginning of the modeling process and must be followed by systematic algorithms for handling the large amount of data, for determining the energies of the particles, and for expressing the results. We have tried to make use of all sources of data ranging from swarm, ion cyclotron resonance, and flow tube techniques at energies below about 10 eV through beam techniques that now extend from fractions of an electron volt to arbitrarily high energies. The intermediate energy range of 1 to 1000 eV is still rarely studied, possibly because very few theoretical calculations of cross sections are available. It is to be hoped that more investigations will be made of the intermediate energy range, including tests of the usefulness of relatively simple theories such as the Born approximation[12] and simple molecular models.

As an illustration of the extremely wide variations in cross sections found in the Ar–H_2 system, we show in Fig. 9 cross sections for Hα excitation taken from this compilation and from Ref. 1. Also shown for comparison is the cross section for electron excitation[70] of Hα. The most striking feature of this data is the larger values of the excitation cross sections for neutral-neutral collisions, such as H + Ar, H_2 + Ar, and H + H_2, compared to ion-neutral collisions, such as H^+ + Ar and H^+ + H_2. While it is dangerous to generalize on the basis of so little data such a behavior is consistent with the other systems we have examined.[1,2] We suggest that the larger cross sections for neutral-neutral collisions result from the ability of the neutrals to penetrate to small internuclear distances where there are more favorable potential curve crossings, while most of the potential energy curves for the ions are repulsive at moderate to small internuclear distances. The large excitation cross sections for H + Ar collisions leads to relatively intense Hα emission from low voltage, low pressure discharges.[6]

In our effort to provide "complete" cross section sets needed for modeling, we have sometimes made arbitrary choices, interpolations, and extrapolations. It is to be hoped that the necessity for estimates of many of the cross sections in critical energy ranges will encourage experimentalists and theoreticians to carry out further work in this area. A "floppy disk" containing the tabulated data is available from the author. Please inform the author of errors, omissions, or new data.

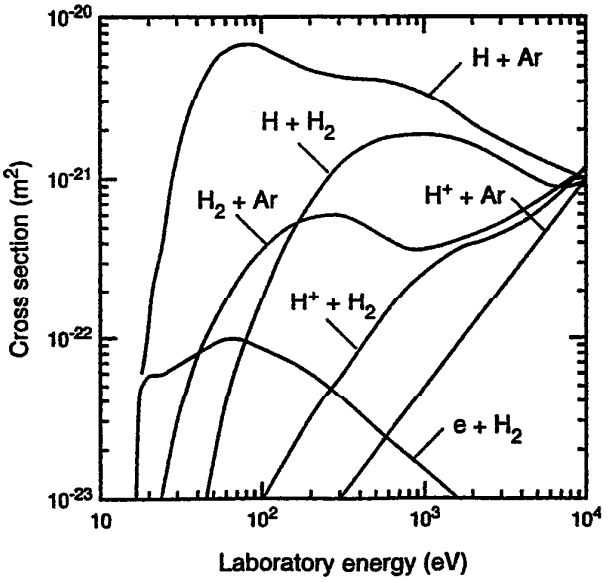

FIG 9. Cross sections for excitation of Hα in collisions of H, H_2, and H^+ with Ar and H_2 versus laboratory energy. Also shown is the cross section for excitation of Hα by electron collisions with H_2 versus electron energy, e + H_2.

13. Acknowledgments

The author wishes to thank B. Van Zyl and W. B. Maier, II for helpful discussions of this work. The author particularly wishes to thank an unknown referee for bringing reference 60 to his attention. This work was supported in part by the National Institute of Standards and Technology.

14. References

[1]A. V. Phelps, J. Phys. Chem. Ref. Data **19**, 653 (1990) and Erratum, J. Phys. Chem. Ref. Data **20**, 1339 (1991). Note that the (M + M) in Eq. (1) should be (m + M).

[2]A. V. Phelps, J. Phys. Chem. Ref. Data **20**, 557 (1991).

[3]E. W. Thomas, *Excitation in Heavy Particle Collisions* (Wiley, New York, 1972), Chap. 9.

[4]B. Van Zyl, H. Neumann, H. L. Rothwell, and R. C. Amme, Phys. Rev. A **21**, 716 (1980).

[5]B. Van Zyl and M. W. Gealy, Phys. Rev. A **35**, 3741 (1987).

[6]B. M. Jelenković, Z. Lj. Petrović, and A. V. Phelps, Bull. Am. Phys. Soc. **36**, 216 (1991).

[7]J. Wagner, Ch. Wild, F. Pohl, and P. Koidl, Appl. Phys. Lett. **48**, 106 (1986); Ch. Wild, J. Wagner, and P. Koidl, J. Vac. Sci. Technol. A **5**, 2227 (1987); Y. Yamashita, H. Toyoda, and H. Sugai, Japan. J. Appl. Phys. **28**, L1647 (1989); Y. Yamashita, K. Katayose, H. Toyoda, and H. Sugai, J. Appl. Phys. **68**, 3735 (1990).

[8]A. E. S. Green and R. J. McNeal, J. Geophys. Res. **76**, 133 (1971).

[9]H. Tawara and A. Russek, Rev. Mod. Phys. **45**, 178 (1973).

[10]H. Tawara, Atomic Data and Nuclear Data Tables **22**, 491 (1978).

[11]A. V. Phelps, in *Abstracts of Contributed Papers for International Conference on the Physics of Electronic and Atomic Collisions*, edited by I. E. McCarthy, W. R. MacGillivary, and M. C. Standage, 1991, p. 539.

[12]E. W. McDaniel, *Collision Phenomena in Ionized Gases* (Wiley, New York, 1964), pp. 19, 71–75.

[13]E. W. McDaniel and E. A. Mason, *The Mobility and Diffusion of Ions in Gases* (Wiley, New York, 1973), p. 344. Note the misprint in Table 7-1-C-1, where the ion listed as H^+ should have been identified as H_3^+.

[14]O. J. Orient, J. Phys. B **4**, 1257 (1971); J. Phys. D **7**, 2266 (1974).

[15]R. L. Champion, L. D. Doverspike, W. G. Rich, and S. M. Bobbio, Phys. Rev. A **2**, 2327 (1970).

[16]M. Abignoli, M. Barat, J. Baudon, J. Fateton, and J. C. Houver, J. Phys. B **5**, 1533 (1972).

[17]J. H. Newman, K. A. Smith, R. F. Stebbings, and Y. S. Chen, J. Geophys. Res. **90**, 11045 (1985); L. K. Johnson, R. S. Gao, C. L. Hakes, K. A. Smith, and R. F. Stebbings, Phys. Rev. A **40**, 4920 (1989).

[18]D. H. Crandall, R. H. McKnight, and D. H. Jaecks, Phys. Rev. A **7**, 1261 (1973).

[19]D. W. Koopman, Phys. Rev. **154**, 79 (1967).

[20]W. B. Maier II, J. Chem. Phys. **69**, 3077 (1978). Note that according to the author the values listed in Table AI of this reference are incorrect and the values in Fig. 7 should be used.

[21]B. Van Zyl, M. W. Gealy, and H. Neuman, Phys. Rev. A **35**, 4551 (1987). See also Ref. 35.

[22]J. S. Risley, F. J. de Heer, and C. B. Kerkdijk, J. Phys. B **11**, 1759 (1978).

[23]W. R. Hess, Phys. Rev. A **9**, 2036 (1974).

[24]J. E. Bayfield, G. A. Khayrallah, and P. M. Koch, Phys. Rev. A **9**, 209 (1974).

[25]D. Jaecks, F. J. de Heer, and A. Salop, Physica **36**, 606 (1967).

[26]M. E. Rudd, Y. K. Kim, D. H. Madison, and J. W. Gallagher, Rev. Mod. Phys. **57**, 965 (1985).

[27]J. A. Phillips, Phys. Rev. **90**, 532 (1953).

[28]C. -L. Liao, R. Xu, G. D. Flesch, M. Baer, and C. Y. Ng, J. Chem. Phys. **93**, 4818 (1990).

[29]R. D. Smith, D. L. Smith, and J. H. Futrell, Int. J. Mass Spectrom. Ion Phys. **19**, 395 (1976).

[30]F. A. Houle, S. L. Anderson, D. Gerlich, T. Turner, and Y. T. Lee, J. Chem. Phys. **77**, 748 (1982).

[31]H. C. Hayden and R. C. Amme, Phys. Rev. **172**, 104 (1968).

[32]J. F. Williams and D. N. F. Dunbar, Phys. Rev. **149**, 62 (1966).

[33]F. von Busch and G. H. Dunn, Phys. Rev. A **5**, 1726 (1972).

[34]Yu. S. Gordeev and M. N. Panov, Zhur. Tekh. Fiz. **34**, 857 (1964) [Sov. Phys. - Tech. Phys. **9**, 656 (1964)].

[35]H. B. Gilbody and J. B. Hasted, Proc. Roy. Soc. (London) **A240**, 382 (1957).

[36]Ch. Ottinger and M. Yang, Z. Naturforsch. **39a**, 1296 (1984).

[37]B. Van Zyl, D. Jaecks, D. Pretzer, and R. Geballe, Phys. Rev. **136**, A1561 (1964).

[38]K. B. McAfee, Jr., D. Sipler, and D. Edelson, Phys. Rev. **160**, 130 (1967).

[39]H. Villinger, J. H. Futrell, F. Howorka, N. Djuric, and W. Lindinger, J. Chem. Phys. **76**, 3529 (1982).

[40]A. A. Prokof'ev, E. S. Zhurkin, L. V. Evseeva, and N. N. Tunitskii, Fiz. Plasmy **4**, 938 (1978) [Sov. J. Plasma Phys. **4**, 525 (1978)].

[41]A. B. Rakshit and P. Warneck, J. Chem. Phys. **74**, 2853 (1981).

[42]W. Lindinger and D. L. Albritton, J. Chem. Phys. **62**, 3517 (1975).

[43]J. H. Whealton, E. A. Mason, and T. H. Vu, Chem. Phys. Lett. **28**, 125 (1974); R. E. Olson and B. Liu, Phys. Rev. A **17**, 1568 (1978).

[44]J. S. Risley, *Electronic and Atomic Collisions*, edited by N. Oda and K. Takayanagi (North-Holland, Amsterdam, 1980) p. 619.

[45]R. L. Champion, L. D. Doverspike, and S. K. Lam, Phys. Rev. A **13**, 617 (1976).

[46]J. S. Risley and R. Geballe, Phys. Rev. A **9**, 2485 (1974).

[47]J. F. Williams, Phys. Rev. **154**, 9 (1967).

[48]J. Geddes, J. Hill, and H. B. Gilbody, J. Phys. B **14**, 4837 (1981).

[49]J. A. Stone and T. J. Morgan, Phys. Rev. A **31**, 3612 (1985).

[50]K. P. Lynch and J. V. Michael, Int. J. Chem. Kinetics **10**, 233 (1978).

[51]A. F. Wagner, G. Das, and A. C. Wahl, J. Chem. Phys. **60**, 1885 (1974).

[52]R. S. Gao, L. K. Johnson, K. A. Smith, and R. F. Stebbings, Phys. Rev. A **40**, 4914 (1989).

[53]B. Van Zyl, T. Q. Le, H. Neumann, and R. C. Amme, Phys. Rev. A **15**, 1871 (1977); H. Neumann, T. Q. Le, and B. Van Zyl, ibid. **15**, 1887 (1977).

[54]W. Aberle, J. Grosser, and W. Krüger, J. Phys. B **13**, 2083 (1980).

[55]A. S. M. Wahby, A. J. H. Boerboom, and J. Los, Physica **75**, 560 (1974); R. C. Ried, J. M. Prausnitz, and T. K. Sherwood, *The Properties of Gases and Liquids* (McGraw-Hill, New York, 1977) 3rd Ed., Chap. 11.

[56]J. H. Kieffer and R. W. Lutz, J. Chem. Phys. **44**, 668 (1966).

[57]M. -M. Audibert, C. Joffrin, and J. Ducuing, Chem. Phys. Lett. **19**, 26 (1973).

[58] J. W. Duff, N. C. Blais, and D. G. Truhlar, J. Chem. Phys. **71**, 4304 (1979): J. M. Hutson and F. R. McCourt, ibid. **80**, 1135 (1984).

[59]S. J. Martin, V. Heckman, E. Pollack, and R. Synder, Phys. Rev. A **36**, 3113 (1987).

[60]V. A. Gusev, G. N. Polyakova, V. F. Erko, Ya. M. Fogel', A. V. Zats, in *Abstracts of Papers for 6th Int. Conf. on the Physics of Electronic and Atomic Collisions*, Edited by I. Amdur (MIT Press, Cambridge, 1969), p. 809.

[61]P. Gaucherel and B. Rowe, Int. J. Mass Spectrom. Ion Phys. **25**, 211 (1977); I. Dotan and W. Lindinger, J. Chem. Phys. **76**, 4972 (1982); C. Rebrion, B. R. Rowe, and J. B. Marquette, ibid. **91**, 6142 (1989).

[62]K. M. Ervin and P. B. Armentrout, J. Chem. Phys. **83**, 166 (1985).

[63]R. C. Amme and J. F. McIlwain, J. Chem. Phys. **45**, 1224 (1966); P. Mahadevan and G. D. Magnuson, Phys. Rev. **171**, 103 (1968).

[64]C. -L. Liao, R. Xu, S. Norbakhsh, G. D. Flesch, M. Baer, and C. Y. Ng, J. Chem. Phys. **93**, 4832 (1990).

[65]A. F. Hedrick, T. F. Moran, K. J. McCann, and M. R. Flannery, J. Chem. Phys. **66**, 24 (1977).

[66]E. Gustafsson and E. Lindholm, Ark. Fys. **18**, 219 (1960).

[67]Ch. Ottinger and M. Yang, Zeit. Phys. A **320**, 51 (1985).

[68]D. Brandt and Ch. Ottinger, Phys. Rev. A **19**, 219 (1979).

[69]C. R. Blakley, M. L. Vestal, and J. H. Futrell, J. Chem. Phys. **66**, 2392 (1977).

[70]G. A. Khayrallah, Phys. Rev. A **13**, 1989 (1976).